Experimental Demonstration of the Role of Anisotropy in Interfacial Pattern Formation

E. Ben-Jacob and R. Godbey
Department of Physics, University of Michigan, Ann Arbor, Michigan 48109

and

Nigel D. Goldenfeld[a]
Institute for Theoretical Physics, University of California, Santa Barbara, California 93106

and

J. Koplik and H. Levine
Schlumberger-Doll Research, Ridgefield, Connecticut 06877

and

T. Mueller and L. M. Sander
Department of Physics, University of Michigan, Ann Arbor, Michigan 48109

We impose anisotropy in modified Hele-Shaw experiments by engraving a grid on one of the plates. Without anisotropy, the dynamics is dominated by tip bifurcations leading to a branched ramified structure. With anisotropy, a dendritic pattern forms, in qualitative agreement with the prediction of recent studies of local growth models.

All manner of interfacial patterns have been observed in various systems and they all seem to differ greatly from each other. For instance, dendritic structures are detected in solidification of a pure undercooled liquid,[1-3] periodic cell structures in directional solidification,[4,5] Saffman-Taylor "fingers"[6] in a Hele-Shaw cell,[7] and self-similar branching structure in electrochemical deposition.[8] In view of the variation in patterns in these systems, no universality in their interfacial dynamics appears to exist. However, we believe that underlying these seemingly unrelated phenomena is a common principle, namely that growth always occurs in two separate ways. Either parabolic dendrites propagate in a way that is governed by anisotropy, or, if the anisotropy is too small, a disorderly behavior dominated by tip splittings results.

A major step toward revealing this principle that governs the dynamics of the systems and the transition from a regime of dendritic dynamics to one of branching dynamics was the development of the geometrical model (GM)[9] and the boundary-layer model (IBM).[10] These are rather simple local growth models inspired by the models of diffusion-controlled solidification. Their simplicity has permitted not only numerical computation[11,12] of the evolution of the interface, but also the elucidation of a new selection mechanism[9,10]: For a given finite anisotropy and low enough undercooling there exists a discrete family of steady-state, shape-preserving, needle-crystal solutions. The selected dendrite is formed by side branches emerging from the needle crystal of highest velocity.[13]

Moreover, in the GM it has been shown[9] that at a critical value of anisotropy (for a given undercooling) all needle-crystal solutions are unstable except the selected one, which is marginally unstable with respect to the tip-splitting mode. At higher anisotropy (for a given undercooling) this mode is stable, and it is unstable below the critical anisotropy. Dendrites are observed in the GM for this specific value of critical anisotropy (for a given undercooling). A similar analysis has not been carried out for the BLM, but there is a nonzero range of anisotropy for which dendritic growth occurs in numerical simulations of the model.[14] Numerical simulations of the BLM and the GM show that below a critical undercooling (for a given anisotropy) the tip evolves by broadening, flattening, and eventually bifurcating into two new tips which continue to evolve in this fashion, giving rise to a succession of tip bifurcations. The experiments which we report here indicate the phase diagram presented in Fig. 1, for interfacial dynamics of diffusion-controlled processes, which is consistent with the results of the local models.

We must bear in mind that the role of anisotropy and the phase diagram outlined above have been demonstrated in local models which are drastic simplifications of the diffusion-controlled solidification, with neglect of interactions between points on the interface which are close in real space but not in terms of their arc-length distance. The GM further neglects memory effects associated with the diffusion field. Thus the question arises: Are long-range memory effects sufficient to give rise to dendritic behavior, or is the presence of anisotropy crucial not only in the GM and the BLM, but in nature as well?[15]

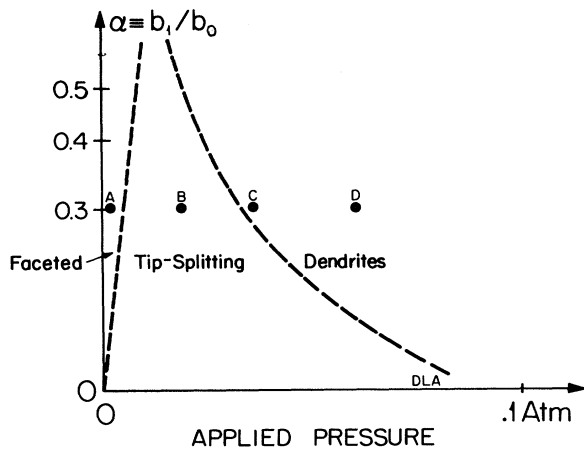The purpose of this paper is to report the first quali-

FIG. 1. Preliminary estimated phase diagram for the Hele-Shaw experiment with anisotropy. The points A,B,C,D indicate the values corresponding to the patterns shown in Fig. 2.

tative experiment to demonstrate the role of anisotropy in interfacial dynamics. Our experiment indicates that these ideas are not an artifact of the approximate nature of the GM and the BLM, but can be a universal feature of interfacial dynamics. To demonstrate the role of anisotropy in interfacial pattern formation we introduce anisotropy in a modified version of a Hele-Shaw experiment by grooving a lattice on one of the plates. Doing so, we observe the formation of dendrites with parabolic tip and side branches similar to those observed in solidification. These are not steady-state solutions, in the sense of having constant growth velocity, but their shape does seem to be time invariant. Moreover, for a given driving force, as we lower the anisotropy we observe tip bifurcations which demonstrate the transition from dendrites to branching as illustrated in Fig. 1. On the basis of our experiments, we postulate the following scenario for the transition from dendritic structure to fractal structure such as seen in diffusion-limited aggregation (DLA)[16]: For a given driving force there is a critical value of the anisotropy below which the tip of the dendrite is unstable with respect to tip bifurcation. Consequently, below the critical value the interfacial dynamics is dominated by tip splitting. As we drive the system further from equilibrium, in the absence of anisotropy, both the period between successive tip bifurcations and the minimum length scale decrease, giving rise to a DLA-like structure in the limit of a very large driving force.[17]

The Saffman-Taylor version of the Hele-Shaw experiment consisted of an interface between two immiscible fluids with different viscosity. The fluids are confined between two parallel closely separated plates. When pressure is applied to the less viscous fluid, the

interface is unstable and known to develop Saffman-Taylor "fingers".[6,18]

The mathematical model describing the dynamics of the interface in a Hele-Shaw cell is the Laplace limit of the full diffusion problem: The velocity field in the viscous fluid is assumed to be two-dimensional and proportional to the pressure gradient as[6]

$$\mathbf{v} = (-b^2/12\eta)\nabla P, \tag{1}$$

where b is the plate separation and η is the viscosity. Similarly, the interface velocity along its outer normal direction (into the viscous fluid) is given by the pressure gradient at the interface. Here we consider the limit of incompressible fluids so that the pressure satisfies the Laplace equation

$$\nabla^2 P = 0. \tag{2}$$

A further assumption that the fluids are immiscible leads to the inclusion of surface tension in the pressure boundary conditions.

At infinity, in the more viscous fluid, $P_\infty = P_0$ where P_0 is the atmospheric pressure. The other boundary condition is P_s, the pressure along the moving interface:

$$P_s = P_1 - d_0\kappa, \tag{3}$$

where P_1 is the applied pressure in the less viscous fluid,[19] d_0 is the isotropic surface tension (in the appropriate units), and κ is the mean curvature of the interface given by

$$\kappa = 1/R_\perp + 1/R_{\parallel}. \tag{4}$$

$R_{\parallel}$ and $R_\perp$ are the radii of curvature of the interface parallel and perpendicular to the plane of the fluid, respectively. Equations (1) and (2), together with the boundary conditions given by Eq. (3), specify the Hele-Shaw model. Note that this system is reminiscent of DLA with finite surface tension.[20] It differs from the models of diffusion-controlled solidification[11] in three aspects: The pressure replaces the temperature field, the diffusion equation is approximated by the Laplace equation, and there is no anisotropy.

Next we describe the results of our version of the Hele-Shaw experiment. The experiment was done by application of pressure at the center of the cell in a manner similar to that of Patterson.[21] We used glycerine (94%) dyed with food color as the viscous fluid and air as the less viscous fluid. The bottom plate is circular with radius 25 cm. On this plate we engraved a regular sixfold lattice of grooves with depth $b_1 = 0.015$ in., width of 0.03 in., and edge-to-edge separation of 0.03 in. We varied the effective anisotropy, α, by changing the spacing b_0 between the two plates; α is then defined by

$$\alpha = b_1/b_0. \tag{5}$$

The typical range is from $\alpha = 0.1$ to $\alpha = 1$. The pressure was applied from a very large (5-gal.) pressure reservoir. The typical range is from $P = 10^{-3}$ atm to $P = 10^{-1}$ atm. In Fig. 1 we show a preliminary estimate of the phase diagram based on the results of the experiment. When the driving force is very small for a given anisotropy α we observe faceted growth [Fig. 2(a)]. The interface includes flat faces that advance one layer at a time via the propagation of kinks. This regime will be described in detail in a forthcoming publication.[22] In the next regime the dynamics of the interface is dominated by the tip-bifurcation instability similar to that observed in the local models [Fig. 2(b)]. We note that in the circular geometry[21] there is no stabilization effect of the walls against tip splitting, in contrast to the case of the channel geometry.[23,24] In our cell we were only able to observe a few tip-splitting bifurcations. We think that in a much larger cell the cascade of tip bifurcations will give rise to a ramified branching structure that will approach a DLA-like fractal dimension on large length scales. In order to show that, we have repeated the experiment without a grooved lattice on the bottom plate. At high pressure we have observed a ramified structure and measured a fractal dimension near to that of DLA[25] ($D \sim 1.7$). This observation gives a qualitative understanding of the fractal dimension of DLA as a limiting process of successive tip bifurcations. In Fig. 2(c) we see the symmetric "snowflake" observed above the tip splitting $\leftrightarrow$ dendritic transition. As we increase the pres-
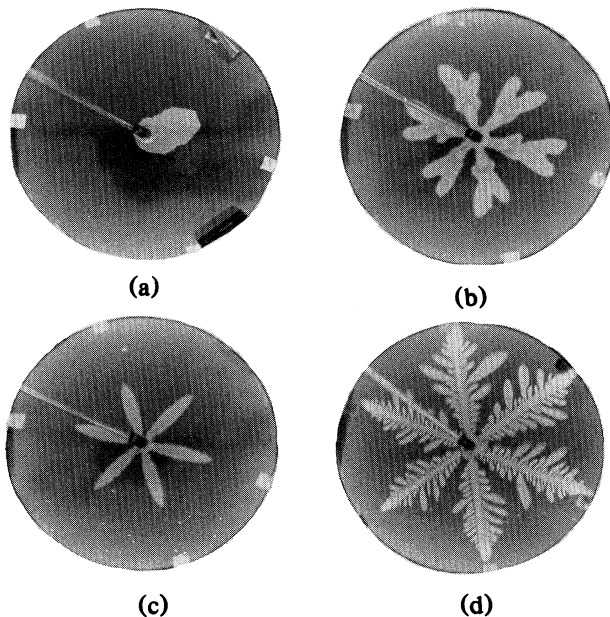

(a)   (b)

(c)   (d)

FIG. 2. The various patterns observed in the Hele-Shaw experiments with anisotropy. (a)–(d) correspond to points (A)–(D) in Fig. 1, respectively, and show (a) faceted growth; (b) tip splitting; (c) needle crystals; (d) dendrites. The plate is 25 cm across.

sure even further we observe the appearance of side branches on the dendrites and the radius of curvature of the tip of the dendrites is reduced [Fig. 2(d)], again in agreement with the prediction of the local models. We emphasize that, as seen in Fig. 2, the size of the dendrites and the spacing between the side branches is not the lattice spacing.

We can carry the analogy between the Hele-Shaw experiment and solidification even further. In order to find a Hele-Shaw analog of direction solidification we have introduced a "lifting version" of the Hele-Shaw experiment. Here, instead of applying pressure to the less viscous fluid, we lift the upper plate at the less viscous side (air, in our experiment) at a given rate. Intuitively, it is clear that by lifting we impose a pressure *gradient* which is analogous to the imposed temperature gradient in directional solidification. To see this, we recall that by the lifting, b in Eq. (1) becomes (at a given time) a function of x—the distance from the pivot—and is of the form

$$b(x) = b_0 + b_0 x/\zeta; \quad x \ll \zeta. \tag{6}$$

Equation (2) is replaced by

$$\nabla^2 P + (2/\zeta)\partial P/\partial x = 0, \tag{7}$$

which is the equation of motion for a difussion process in a frame moving with velocity $2D/\zeta$, where D is the diffusion constant. $R_\perp$ in Eq. (4) has the following x dependence:

$$R_\perp = c/b(x) \cong (c/b_0)(1 - x/\zeta), \tag{8}$$

where c and b_0 are constants, so that the pressure at the interface [Eq. (3)] becomes

$$P_s = P_1 - d_0 b_0/c - d_0/R_{\parallel} - (d_0 b_0/c\zeta)x. \tag{9}$$

These equations have the same form as the equations describing directional solidification in the quasistatic limit.[5] In Fig. 3 we show some results of the interfacial dynamics in the lifting experiment.

In this experiment we have used a bottom plate with a square lattice grooved on it, with grooves of width 0.03 in. and depth 0.015 in., separated by 0.03 in. We control the velocity of lifting by using a variable-speed motor. In Fig. 3(a) we show the resulting "fingers" at low velocity[26] (about 0.5 cm/sec; the scale is 20 cm). As we increase the velocity (by increasing the rate of lifting) we observe the array of dendrites shown in Fig. 3(b). The spacing of the dendrites depends on the lifting rate—faster lifting gives smaller spacing—and on the initial plate spacing. The velocity is about 15 cm/sec and the wavelength is about 2 cm. Finally, we emphasize that, similarly to the previous experiment, in the absence of anisotropy the interface dynamics is dominated by tip bifurcations. The resulting pattern is shown in Fig. 3(c) (the portion shown is of width 20 cm). We note that for small anisotropy (large spacing) we observe patterns similar to those of the numerical simulations of Vicsek[27] and Jensen.[28] We claim that
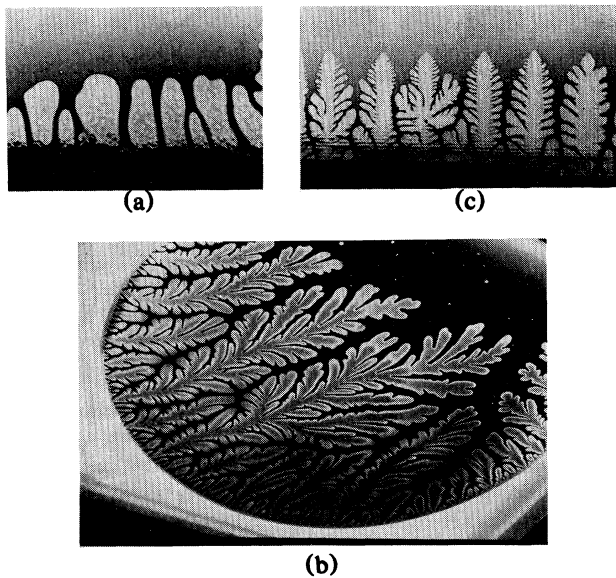
(a)

(c)

(b)

FIG. 3. The lifting Hele-Shaw experiment. (a) "Fingers" at low velocity. (b) Branched "fingers" at higher velocity. (c) Array of dendrites with imposed anisotropy.

the use of a square lattice in the simulations in these references provided weak anisotropy.

In summary, we have described qualitative experiments which demonstrate the role of anisotropy in interfacial pattern formation. This experiment proves that anisotropy is truly essential to the formation of dendrites and not an artifact arising from the approximate nature of the local models.[11,12] Other experiments, which study the effect of impurities on the tip bifurcation instability and impose anisotropy by use of liquid crystals as viscous fluids, are in progress. Quantitative detailed measurements of the phase diagram will be reported in a forthcoming publication.[22]

(a)Present address: Department of Physics, University of Illinois, Urbana, Ill. 61801.

[1]M. E. Glicksman, R. J. Shaefer, and J. A. Ayers, Metall. Trans. A 7, 1747 (1976).

[2]T. Fujioka, Ph.D. thesis, Carnegie-Mellon University, 1978 (unpublished).

[3]J. S. Langer, Rev. Mod. Phys. 52, 1 (1980).

[4]L. A. Tarshis, J. L. Walker, and J. W. Ratter, in Metallography, Structures and Phase Diagrams, edited by M. B. Bauer (American Society for Metals Novelty, 1983).

[5]D. J. Wollkind and L. A. Segel, Trans. Roy. Soc. Edinburgh 51, 268 (1970).

[6]P. G. Saffman and G. I. Taylor, Proc. Roy. Soc. London, Ser. A 245, 312 (1958).

[7]H. S. S. Hele-Shaw, Nature 58, 34 (1898).

[8]M. Matsushita, M. Sano. Y. Hayakawa, H. Honjo, and Y. Sawada, Phys. Rev. Lett. 53, 286 (1984); R. Brady and R. C. Ball, Nature 309, 225 (1984).

[9]D. Kessler, J. Koplik, and H. Levine, Phys. Rev. A 31, 1712 (1985).

[10]E. Ben-Jacob, N. D. Goldenfeld, B. G. Kotliar, and J. S. Langer, Phys. Rev. Lett. 53, 2110 (1984).

[11]E. Ben-Jacob, N. D. Goldenfeld, J. S. Langer, and G. Schön, Phys. Rev. Lett. 51, 1930 (1983), and Phys. Rev. A 29, 330 (1984).

[12]R. Brower, D. Kessler, J. Koplik, and H. Levine, Phys. Rev. Lett. 51, 1111 (1983), and Phys. Rev. A 29, 1335 (1984); D. Kessler, J. Koplik, and H. Levine, Phys. Rev. A 30, 3161 (1984).

[13]For a given anisotropy, there is a critical undercooling below which there is no needle-crystal solution.

[14]The study of the stability of the needle-crystal solutions in the BLM is in progress. Preliminary results show that all solutions in the discrete family are unstable. The one with the largest velocity is the least unstable. The dendrites that have been observed are not transient since they maintain their tip velocity and tip curvature.

[15]Some additional qualitative evidence is given by a numerical simulation of the diffusion system in the zero–Peclet-number limit, where anisotropy was found to be required for tip stabilization: D. Kessler, J. Koplik, and H. Levine, Phys. Rev. A 30, 2820 (1984).

[16]T. A. Witten, Jr., and L. M. Sander, Phys. Rev. Lett. 47, 1400 (1981), and Phys. Rev. B 28, 5686 (1983).

[17]The structure has a minimum length scale determined by the surface tension and the driving force. However, the skeleton has a DLA-like structure. As we drive the system further from equilibrium it shrinks to its limiting skeleton.

[18]G. Tryggvason and H. Aref, J. Fluid Mech. 136, 1 (1983).

[19]We assume constant pressure in the less viscous fluid. This assumption is analogous to the assumption of no diffusion in the solid in diffusion-controlled solidification.

[20]L. Patterson, Phys. Rev. Lett. 52, 1621 (1984); L. Kadanoff, to be published; C. Tang, to be published.

[21]L. Patterson, J. Fluid Mech. 113, 513 (1981).

[22]E. Ben-Jacob, R. Godbey, N. D. Goldenfeld, and T. Mueller, unpublished.

[23]D. Kessler and H. Levine, to be published.

[24]D. Ben-Simon, private communication.

[25]Ramified structures in a Hele-Shaw experiment have been recently observed also by J. Nittmann, G. Daccord, and H. E. Stanley, Nature 314, 141 (1985).

[26]R. J. Fields and M. F. Ashby, Philos. Mag. 33, 33 (1976).

[27]T. Vicsek, Phys. Rev. Lett. 53, 2281 (1984).
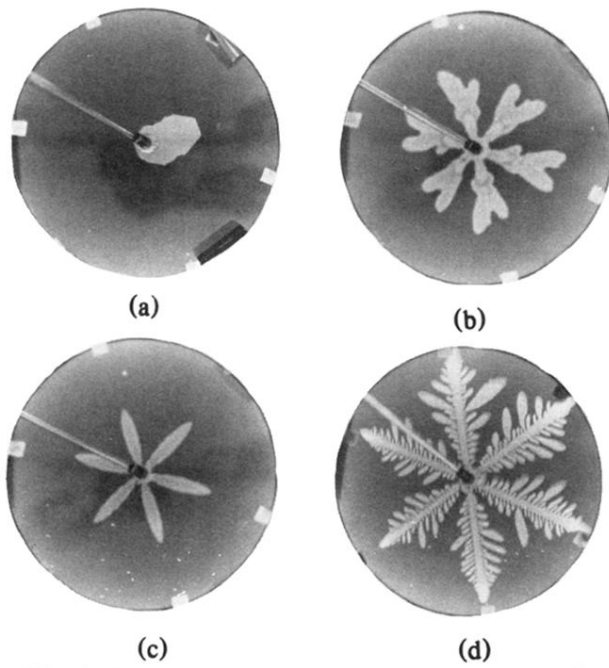
[28]J. Jensen, unpublished.

FIG. 2. The various patterns observed in the Hele-Shaw experiments with anisotropy. (a)–(d) correspond to points (A)–(D) in Fig. 1, respectively, and show (a) faceted growth; (b) tip splitting; (c) needle crystals; (d) dendrites. The plate is 25 cm across.
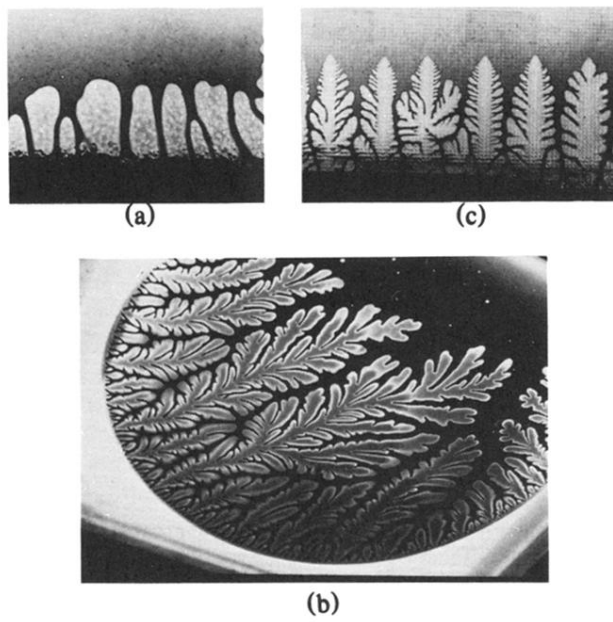
FIG. 3. The lifting Hele-Shaw experiment. (a) "Fingers" at low velocity. (b) Branched "fingers" at higher velocity. (c) Array of dendrites with imposed anisotropy.